Supporting Information

Electron transfer bridge inducing polarization of nitrogen molecule for enhanced photocatalytic nitrogen fixation

Huiyi Li[†,§], Jiongrong Wang[‖,§], Zhoushilin Ruan[†,§], Pengfei Nan,[§] Binghui Ge,[§] Ming Cheng[†], Lan Yang[†], Xiaohong Li[†], Qilong Liu[‡], Bicai Pan[†], Qun Zhang[†,*], Chong Xiao[†,‡,*] and Yi Xie[†,‡,*]

[†]Hefei National Research Center for Physical Sciences at the Microscale, Collaborative Innovation Center of Chemistry for Energy Materials (iChEM), University of Science and Technology of China, Hefei, Anhui 230026, China

[‖] Key laboratory of Strongy-Coupled Quantum Matter Physics, Department of Physics University of Science and Technology of China, Hefei, Anhui 230026, People's Republic of China.

[‡] Institute of Energy, Hefei Comprehensive National Science Center, Hefei, Anhui, 230031, China

[§] Key Laboratory of Structure and Functional Regulation of Hybrid Materials of Ministry of Education, Institutes of Physical Science and Information Technology, Anhui University, Hefei 230601, China

Corresponding authors: E-mail: qunzh@ustc.edu.cn; cxiao@ustc.edu.cn; yxie@ustc.edu.cn

Experimental Section

All the chemicals were of analytical grade purity and used as received without further purification.

Synthesis

Bismuth nitrate pentahydrate ($Bi(NO_3)_3 \cdot 5H_2O$), Polyvinyl Pyrrolidone (PVP), and Sodium chloride (NaCl) were obtained from Sinopharm Chemical Reagent Co., Ltd, Cerium chloride heptahydrate($CeCl_3 \cdot 7H_2O$) were obtained from Aladdin. All chemicals were used as received without further purification. In a typical synthesis, 0.486 g $Bi(NO_3)_3 \cdot 5H_2O$ and 0.2 g PVP were dissolved in 25 mL Ethylene Glycol (EG) with vigorous stirring for 30 min. Then, 5 mL of saturated NaCl solution was slowly added to the above mixture, yielding a uniform white suspension. After another 30 min of agitation, the mixture was transferred into a Teflon-lined stainless-steel autoclave and then heated at 160 °C for 24 h. Adjusting the Ce content to 0, 11.2 mg, 18.7 mg, 29.8 mg, 37.3 mg, and 56.0 mg to prepare pure BiOCl, Ce-BiOCl-1, Ce-BiOCl-2, Ce-BiOCl-3, Ce-BiOCl-4, and Ce-BiOCl-5 samples. Naturally cooled to room temperature, the precipitates were washed with absolute alcohol and deionized water six times and dried at 60 °C in air.

Characterizations

The X-ray diffraction (XRD) patterns were recorded on a Philips X'Pert Pro Super diffractometer with Cu Kα radiation (λ = 1.54178 Å). The transmission electron microscopy (TEM) images were obtained using Hitachi-7700 operated at an acceleration voltage of 100 kV. The X-ray photoelectron spectra (XPS) were collected on a Thermo-Fisher ESCALAB 250Xi with Mg Kα (hν = 1253.6 eV) as the excitation source. The C 1s line was referenced to 284.8 eV to correct the carbon signal. Atomic force microscopy (AFM) image in the present work was detected using HITACHI

AFM5500M. The ultraviolet-visible (UV-vis) spectra were recorded on a PerkinElmer Lambda 950 UV−vis−NIR spectrophotometer. The *in-situ* diffuse Fourier transform infrared (FTIR) spectra were performed by a Bruker 66V FTIR spectrometer with a specific reaction cell. Raman spectra were recorded on Horiba Xplora Plus Raman spectrometer system. using a He/Ne laser (532 nm) as the excitation source at room temperature and diffraction grating of 1800 grooves/mm. For the gas Raman characterization, the nitrogen was pumped into a homemade gas Raman cell. The scattered radiation was collected in the direction perpendicular to the direction of laser-radiation propagation.

Photocatalytic N_2 Fixation Measurements

The photocatalytic N_2 fixation experiments were carried out in an N_2 atmosphere at room temperature. Typically, 10 mg of the sample was dispersed in 100 mL of water in the reactor. Before the nitrogen reduction, the catalyst powder was dispersed into 40 mL of water and then irradiated under a 300 W Xe lamp for 5 h to eliminate any surface organic. Then the catalyst was collected by centrifuge and used for futher test. The sample was sonicated to form a uniform suspension and stirred in the dark with pure N_2 bubbled for 30 min. Subsequently, the suspension was irradiated by a Xe lamp (CEL-HXF300, Beijing China Education Au-light Co., Ltd) equipped under full-spectrum with a power density of 200 mW cm^{-2}. After stopping light irradiation, the reaction solution was collected by a syringe, from which the catalyst was removed through centrifugation. The NH_4^+ and NO_3^-concentration were detected by using an ion chromatograph (IC, Dionex Aquion, CS16) after filtration with a 0.22 μm membrane. The N_2H_4 present in the solution was determined by the method of Watt and Chrisp. The p-$C_9H_{11}NO$ (5.99 g), HCI (30 mL), and C_2H_5OH (300 mL) were mixed and used

as a color reagent. In detail, 5 mL reaction solution was added into 5 mL prepared color reagent and stirred for 15 min at 25 °C.

Isotopic testing in photocatalytic N_2 fixation.

The isotopic experiment is similar to the above photocatalytic N_2 fixation measurement, but the difference is that the high-purity $^{15}N_2$ gas replaces the high-purity $^{14}N_2$ in this experiment. Then, the above-mentioned reactor was illuminated for 4h. To test $^{15}NH_4^+$ products, 10 mL of the above mixture was extracted from the reactor and centrifuged to remove the catalyst. The above collected mother liquor was further condensed to 0.5 mL and added 55 μL HCl (1 M). After that, above concentrate was added to 0.1 mL DMSO-d_6 and then tested in an NMR spectrometer (Bruker, 400M).

Quasi-in situ XANES measurements.

Near Edge X-ray Absorption Fine Structure (NEXAFS) was carried out at the Catalysis and Surface Science Endstation at the BL11U beamline in the National Synchrotron Radiation Laboratory (NSRL) in Hefei, China. This beamline is connected to an undulator and equipped with two gratings that offer soft X-rays from 20 to 600 eV with a typical photon flux of 5×10^{10} photons/s and a resolution($E/\Delta E$) better than 10^5 at 29 eV. This system is comprised of four ultrahigh vacuum (UHV)chambers including an analysis chamber, preparation chamber, molecular beam epitaxy (MBE) chamber, and a radial distribution chamber. The base pressures are7×10^{-11}, 1×10^{-10}, $5\times10^{-10}$and 2×10^{-11} mbar, respectively. A sample load-lock system is connected to the sample transfer chamber. The analysis chamber is equipped with a VG Scienta R4000 analyzer, a monochromatic Al *Ka* X-ray source, a UV light source, low energy electron diffraction (LEED), a flood electron gun, and a manipulator with high precision and five-degree-of-freedom. The preparation chamber comprises an ion gun, a quartz crystal microbalance (QCM), a residual gas analyzer, a manipulator with high precision

and four-degree-of-freedom, and several evaporators. The MBE chamber houses a QCM, several evaporators, and a manipulator with two-degree-of-freedom. With this radial distribution chamber, the time for each transfer process between the two chambers is less than 1 minute. In this work, BiOCl and Ce-BiOCl samples were exposed to flowing N_2 for 30 min in the high-pressure reactor under 1 atm and then transferred to the analysis chamber for Quasi situ XANES measurements.

Photoelectrochemical measurement.

In a typical process, 10 mg catalyst was dispersed in 1 mL absolute ethanol and 5 uL Nafion by sonication for 30 min. Then, 10 μL of the suspension was drop-coated at FTO glass with an area of 1 × 1 cm^2. The FTO glasses were dried at 80 ^oC for 24 h to remove volatile organic compounds before use. The Ag/AgCl electrode and a platinum plate were used as the reference electrode and the counter electrode, respectively. The prepared FTO/sample was used as the working electrode with 0.5 M Na_2SO_4 aqueous solution as the electrolyte. The electrochemical impedance spectroscopy (EIS) spectra were acquired in the same three-electrode system by tuning the frequency range of 0.1 to 100 kHz under open circuit potential. All the photoelectrochemical measurements were performed on a CHI 760E electrochemical workstation (CHENHUA, China).

Ultrafast transient absorption measurements.

The femtosecond time-resolved transient absorption (fs-TA) measurements were performed on a pump-probe system (Helios, Ultrafast Systems LLC) in combination with an amplified femtosecond laser system (Coherent) under ambient conditions. The 320 nm pump pulses (~100 nJ/pulse at the sample, corresponding to a pump fluence of ~140 μJ/cm^2 given the typical focus radii of ~150 μm) were delivered by an optical parametric amplifier (TOPAS-800-fs), which was excited by Ti: sapphire regenerative amplifier (Legend Elite-1K-HE; center wavelength 800 nm, pulse duration 35 fs, pulse

energy 3 mJ, repetition rate 1 kHz) seeded with a mode-locked Ti: sapphire laser system (Micra 5) and pumped with a 1-kHz Nd: YLF laser (Evolution 30). The white-light-continuum (WLC) probe pulses were generated by focusing 800 nm beam (split from regenerated amplifier with a tiny portion) onto a sapphire plate. A reference beam split from WLC was used to correct the pulse-to-pulse fluctuation of the WLC for achieving the best signal-to-noise ratio. The time delay (0–8 ns) between the pump and probe pulses was varied by a motorized optical delay line. The instrument response function (IRF) was determined to be ~100 fs by a routine cross-correlation procedure. A mechanical chopper operating at 500 Hz was used to modulate the pump pulse such that the TA spectra with and without pump pulses can be recorded alternatively. The temporal and spectral profiles (chirp-corrected) of the pump-induced differential transmission of the WLC probe light (i.e., absorbance change) were visualized by an optical fiber-coupled multichannel spectrometer (with a CMOS sensor) and further processed by the Surface Xplorer software. The material samples were first well dispersed in ethylene glycol (1 mg/mL), and then two drops of the dispersions were placed as uniformly as possible onto the surface of quartz plates. Subsequently, the quartz plates with sample dispersions were heated at 60 °C for 60 min in a vacuum oven and then cooled down naturally to room temperature, yielding the uniform film of the investigated samples.

DFT calculations.

All calculations in this article are performed using VASP (Vienna *ab initio* simulation package) based on Density Functional Theory (DFT)+*U*. The electron-ion interaction is described by Projector Augmented Wave (PAW) potentials, and the exchange-correlation energy function is represented using the generalized gradient approximation (GGA) in the Perdew–Burke–Ernzerhof (PBE) form. To simulate the doping of Ce in

the surface region of the BiOCl material, a (2×2) supercell of the BiOCl slab with (001) surface is chosen, which is composed of 11 atomic layers and on which the Ce is deposited on the top of the Bi atom in the surface. And a vacuum region of 20 Å along the direction perpendicular to the surface was applied to avoid the interaction between the surface and its images. In our calculations, the kinetic energy cutoff for the plane-wave basis set is 520 eV and the Brillouin zone is sampled with 2×2×1 *k* points. During the optimizations, structures were relaxed until an energy convergence of 10^{-5} eV per atom and a force convergence of 0.02 eV $Å^{-1}$ are reached. In addition, the spin polarization and the van der Waals correction are considered in calculations.

Results and Discussion:

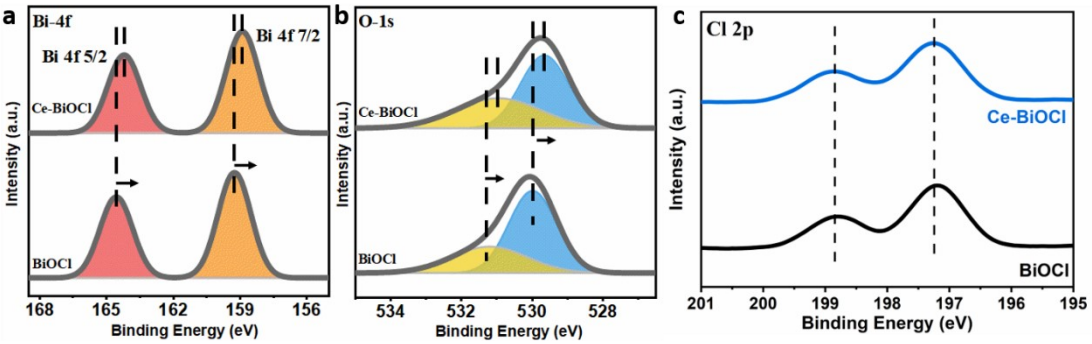

Figure S1. (a) Bi 4f XPS (b) O 1s spectra and (c) Cl 2p spectra of BiOCl and Ce-BiOCl.

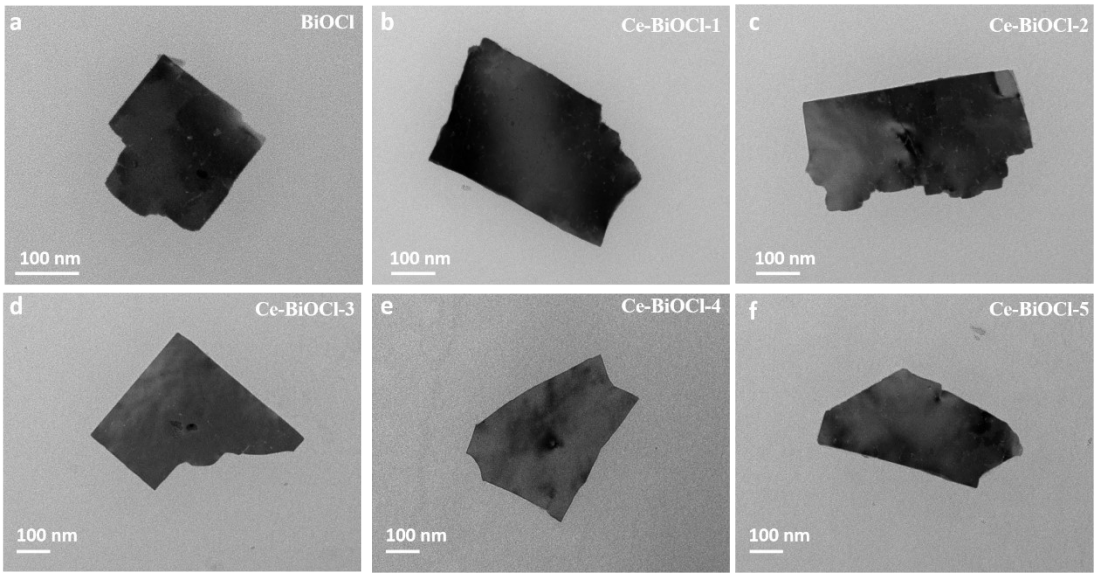

Figure S2. TEM images of (a) BiOCl, (b) Ce-BiOCl-1; (c) Ce-BiOCl-2; (d) Ce-BiOCl-3; (e) Ce-BiOCl-4; (f) Ce-BiOCl-5.

Figure S3. TEM characterization of Ce-BiOCl nanomaterial at a large scale

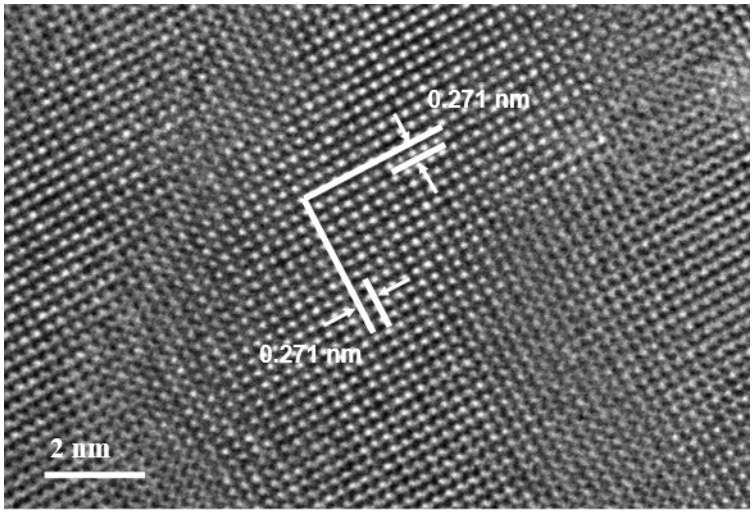

Figure S4. HRTEM image of BiOCl.

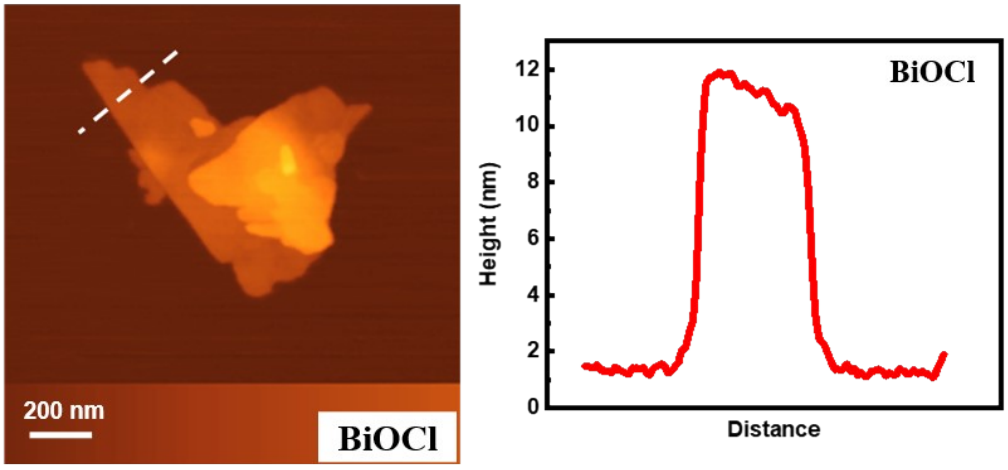

Figure S5. AFM image and corresponding height image of BiOCl.

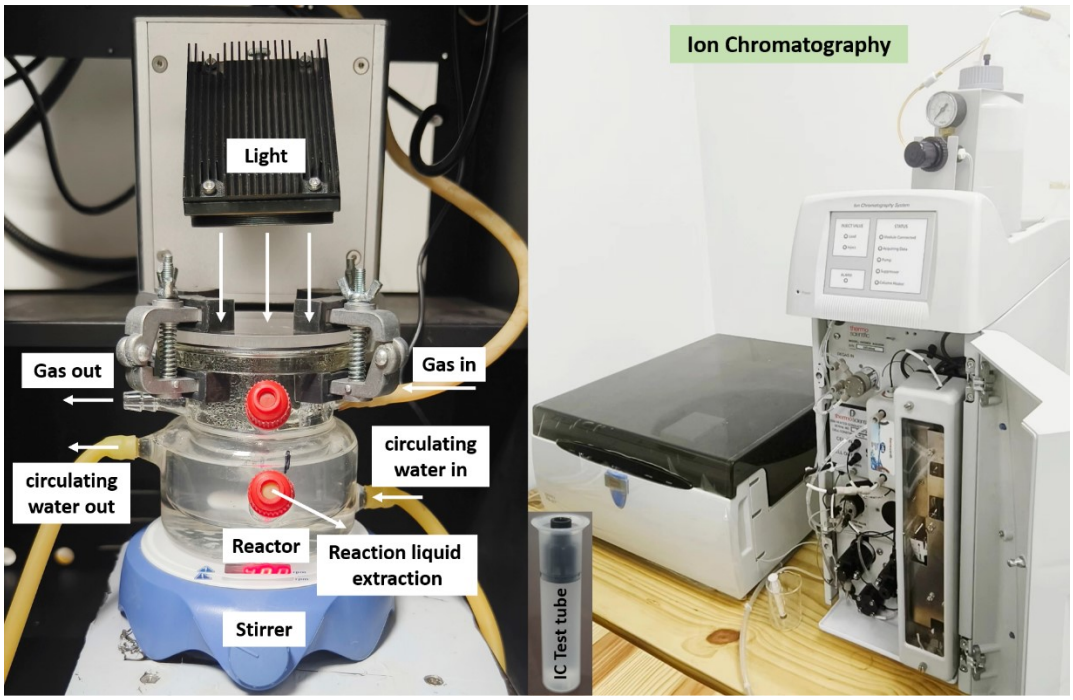

Figure S6. The reaction equipment and testing equipment of the nitrogen photofixation process.

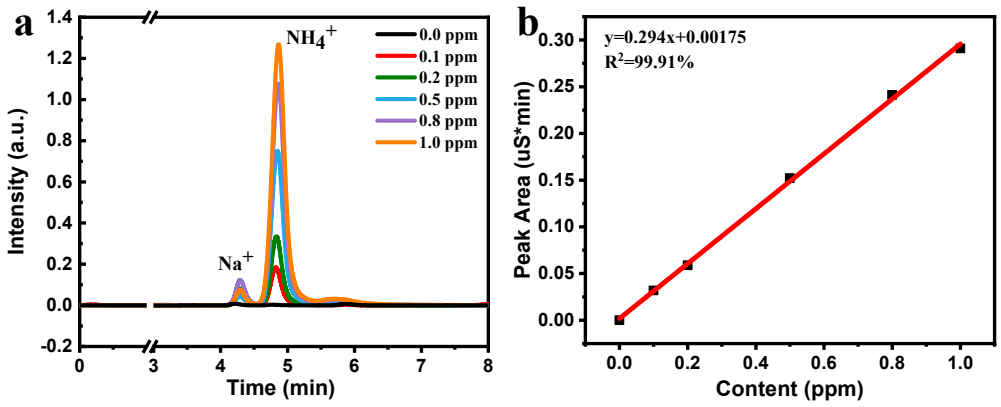

Figure S7. (a) Measurement curves of NH_4^+ from 0.0 ppm to 1 ppm tested by the ion chromatography; (b) The standard curves of NH_4^+ obtained from the Ion Chromatography.

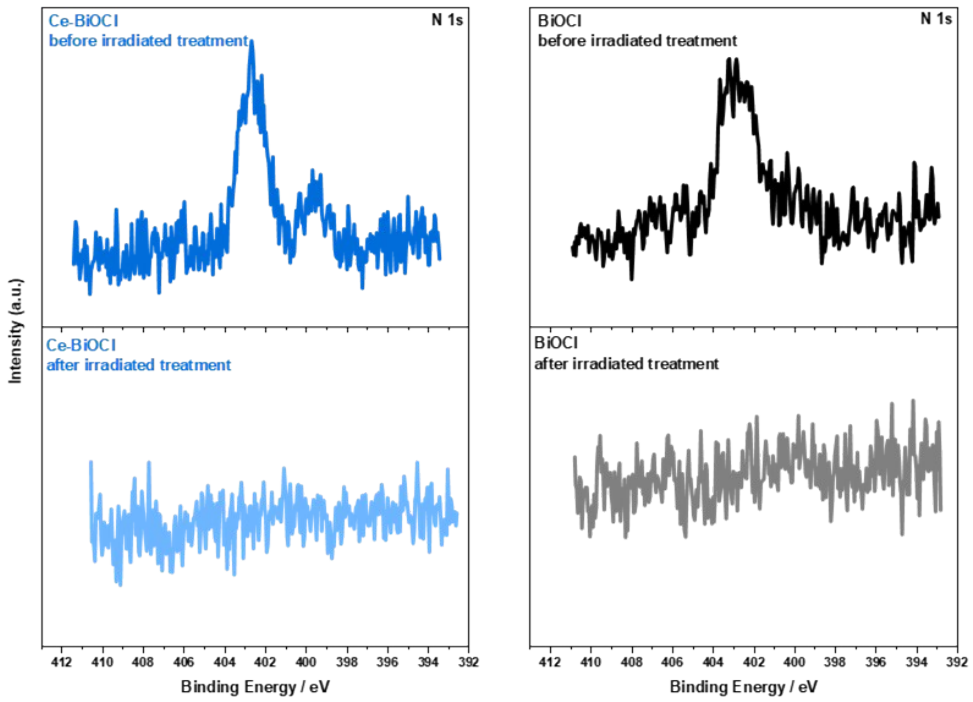

Figure S8. N 1s XPS of Ce-BiOCl and BiOCl before and after irradiation for 5 h in water.

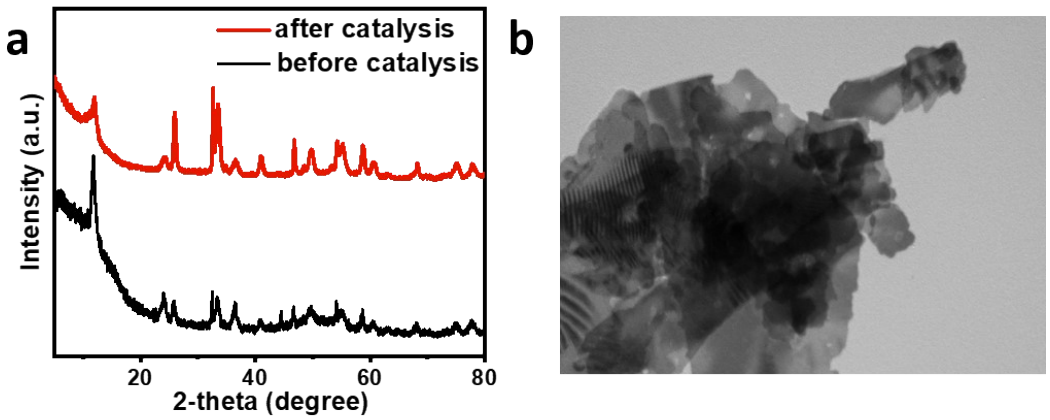

Figure S9. Characterizations for the Ce-BiOCl nanosheets after photocatalytic (a) XRD patterns; (b) TEM image.

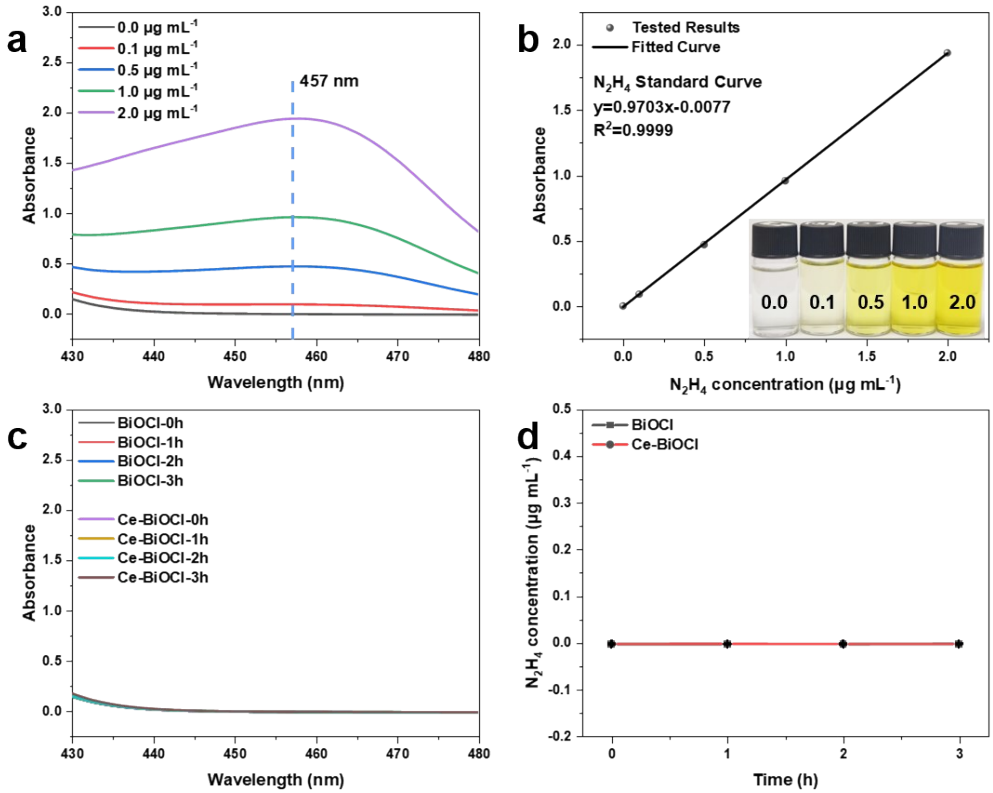

Figure S10 (a) UV-vis absorbance curves of chromogenic solution with pre-set N_2H_4. concentrations after 15 min stirring at room temperature. b) Standard calibration curve for N_2H_4. The inset in (b) shows the photograph of chromogenic solution under various N_2H_4 concentrations. (c) UV-vis absorbance curves of chromogenic solution with the filtered solution from BiOCl and Ce-BiOCl photocatalytic N_2 reduction reaction under different time.(d) The concentration of photocatalytic N_2 reduction to N_2H_4 for BiOCl and Ce-BiOCl catalyst as detected using the Watt and Chrisp method.

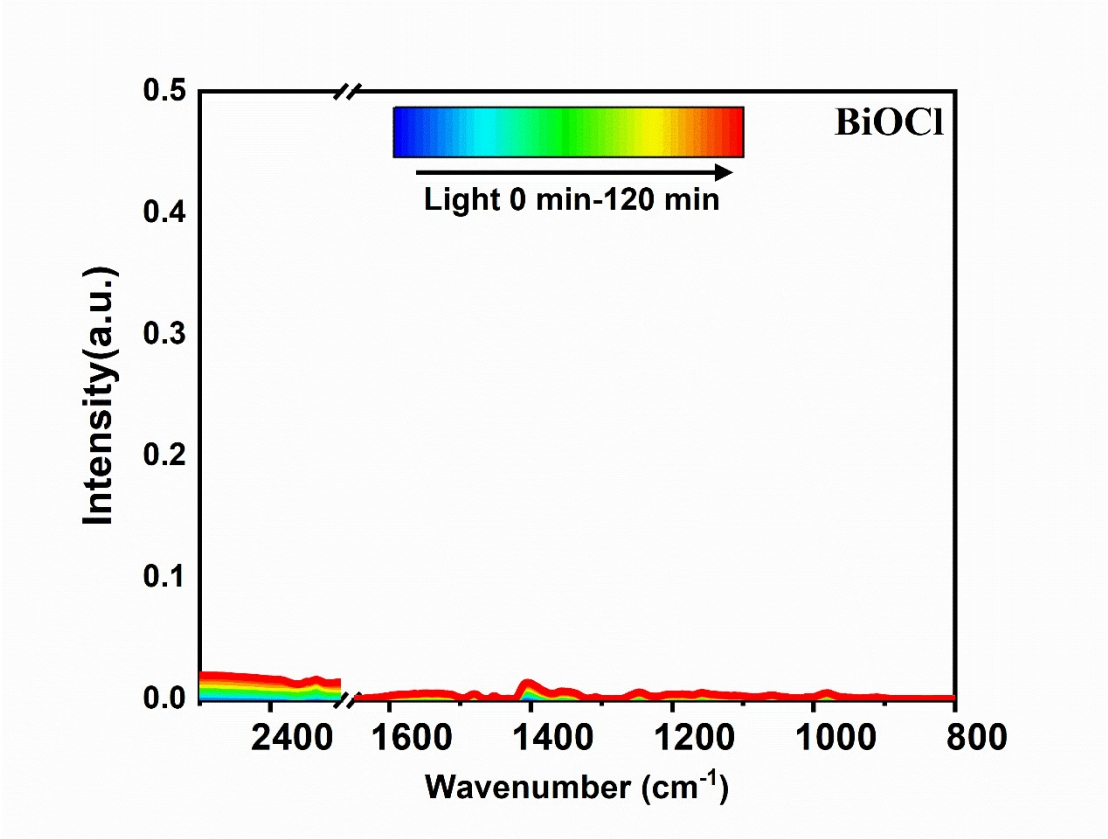

Figure S11. In-situ DRIFTS for the N_2 reduction process on the BiOCl.

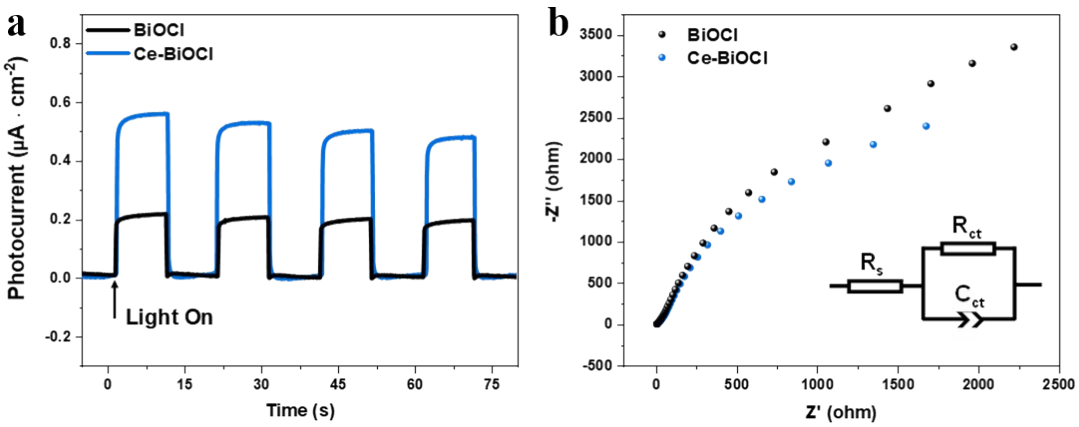

Figure S12. (a) The time-dependent photocurrent response of BiOCl and Ce-BiOCl; (b) EIS of the as-prepared BiOCl and Ce-BiOCl photocatalysts.

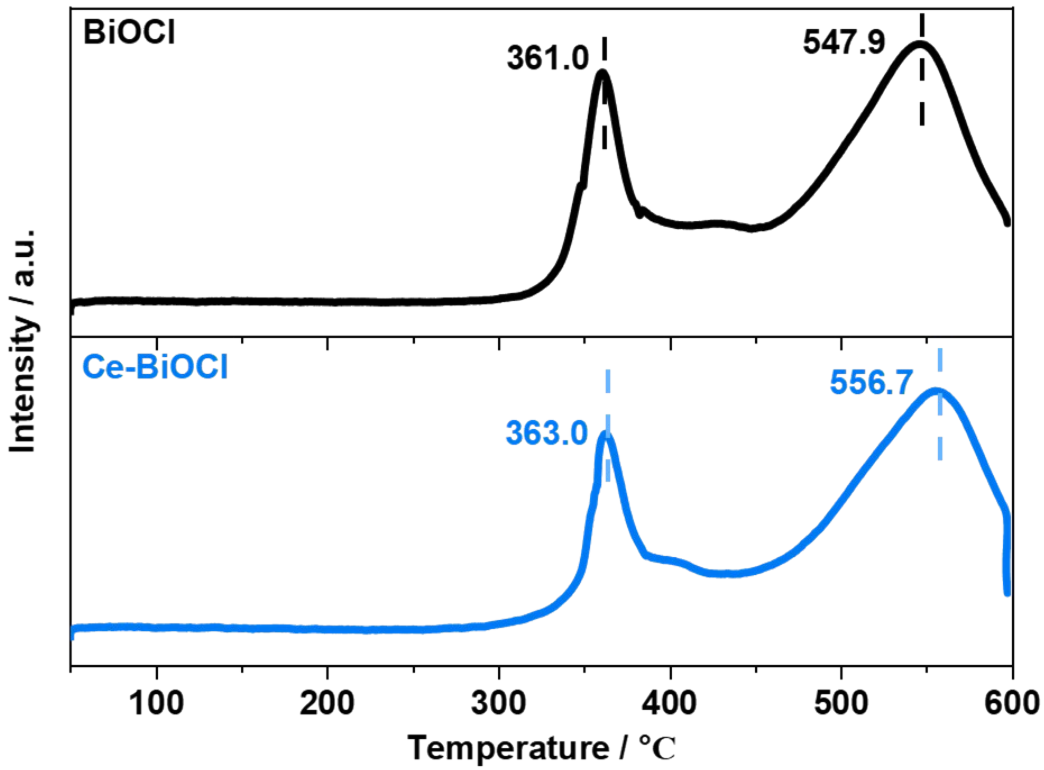

Figure S13. N_2-TPD profiles for the BiOCl and Ce-BiOCl.

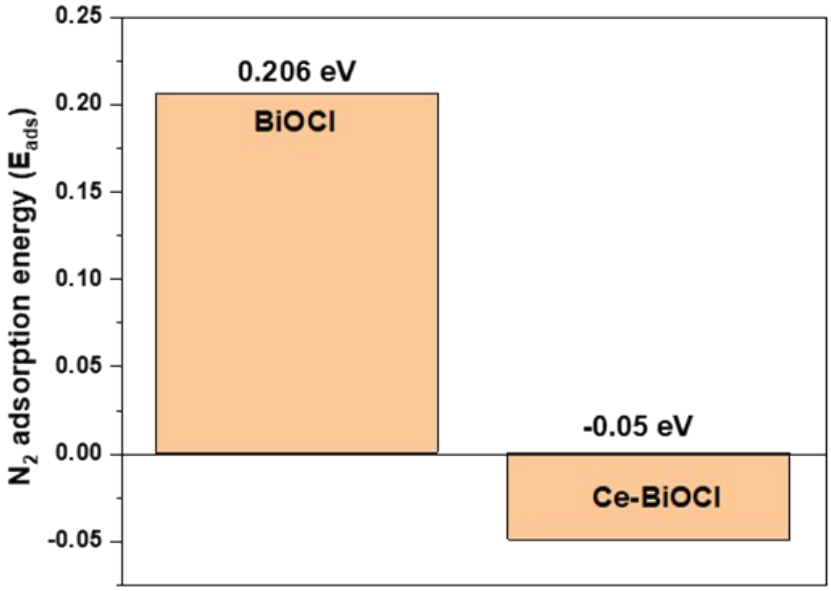

Figure S14. The calculated N_2 adsorption energy (E_{ads}) of BiOCl and Ce-BiOCl.

3. Tables

Table S1. Ammonia production of Ce-BiOCl under various reaction conditions.

	Catalyst	Light	Atmosphere	NH_4^+ production (μmol h^{-1} g^{-1})
1	✓	✓	**N_2**	**46.7**
2	✓	✓	**Ar**	**n.d.[a]**
3	✓	✓	**He**	**n.d.**
4	×	✓	**N_2**	**n.d.**
5	✓	×	**N_2**	**n.d.**

[a] n.d. stands for not detected.

Table S2. Bader charge analysis (Number of electrons/valence electrons per atom) of BiOCl and Ce-BiOCl.

Atom	BiOCl	Ce-BiOCl
$\mathbf{Bi_1}$	13.27/15	13.20/15
$\mathbf{Bi_2}$	13.26/15	14.17/15
$\mathbf{N_d}$	5.09/5	5.35/5
$\mathbf{N_p}$	5.26/5	5.17/5

Table S3. Summary of the photocatalytic ammonia evolution performance of some BiOX-based catalysts.

Catalysts	**scavenger**	**Detecting Method**	**Product rate (μmol h^{-1} g^{-1})**	**Ref**
Ce-BiOCl	none	IC	46.7	This work
BiOCl-OVs	none	IC	0.77	J. Am. Chem. Soc. 2020, 142, 7574-7583
BiOCl (010)	none	Nessler's reagent	67.5	Nanoscale, 2016, 8, 1986
Fe-BiOCl	none	Nessler's reagent	30	Journal of Colloid and Interface Science 584: 174-181
$ZnIn_2S_4$/BiOCl	none	Nessler's reagent	14.6	Catalysts 2019, 9, 729
MoO_2/BiOCl	none	Nessler's reagent	35	ChemCatChem 2019, 11, 6467
BiOBr-OVs	none	Nessler's reagent	49.4	Nano Lett. 2018, 18, 7372−7377
BiOBr, exposed {001} facets	none	Nessler's reagent	104.2	J. Am. Chem. Soc. 2015, 137, 6393.
Bi_2Te_3/BiOCl	0.02M MeOH	Nessler's reagent	315.9	Catal. Commun. 2018, 116, 16.

$Bi_4O_5Br_2$/ZIF-8	none	Indophenol blue method	327.33	Chem. Eng. J. 2019, 371, 796.
Bi_2MoO_6/OV–BiOBr	none	Nessler's reagent	90.7	Nanoscale, 2019,11, 10439-10445
H-Bi_5O_7I microspheres	none	Nessler's reagent	162.48	Dalton Trans. 2020, 49, 9123
C-BiOI	10% EtOH	Nessler's reagent	311	J. Colloid Interface Sci. 2019, 539, 563.
Bi_5O_7Br	none	Nessler's reagent	1380	Adv. Mater. 2017, 29, 1701774
BiOCl-Fe%	none	Indophenol blue method	1022.4	ACS Appl. Energy Mater. 2019, 2, 8394−8398 Letter
Bi_5O_7Br-40	none	Nessler's reagent	12720	J. Am. Chem. Soc. 2020, 142, 12430
GQDs/g-C_3N_4/BiOCl	10% MeOH	Indophenol blue method	1773.8	*Int J Energy Res*. 2022; 46(9): 12147- 12159
Cu_2O@BiOCl	none	Nessler's reagent	181.9	*Inorg. Chem.* 2022, 61, 16, 6045–6055
CoOOH/BiOCl	none	Indophenol blue method	140	*Materials Today Chemistry, 2022, 24, 100993*